Fermi National Accelerator Laboratory

FN-522

Non Ionizing Energy Deposition in Silicon for Radiation Damage Studies

A. Van Ginneken
Fermi National Accelerator Laboratory
P.O. Box 500, Batavia, Illinois 60510

October 1989

Operated by Universities Research Association, Inc., under contract with the United States Department of Energy

Non Ionizing Energy Deposition in Silicon for Radiation Damage Studies

A. Van Ginneken
Fermi National Accelerator Laboratory*
P. O. Box 500, Batavia, IL 60510

October 1989

Abstract

The non-ionizing dE/dx of protons, neutrons, pions, photons, electrons, and muons in silicon is calculated as a function of energy for application in studies of radiation damage.

1 Introduction

Building on the work of, among others, Simon et al. [1] and Van Lint et al., [2] Burke, Dale, Summers, and co-workers [3, 4] have concluded that to good approximation the displacement radiation damage in silicon is proportional to the non-ionizing energy deposited by energetic nuclear recoils. Ref. [4] presents a graph of the non-ionizing energy loss per unit of target thickness in a thin silicon target produced by protons, neutrons, and electrons (above 1 MeV) as a function of particle energy. This type of information is easy to incorporate into CASIM [5] or other Monte Carlo simulations of hadronic and electromagnetic showers and allows one to estimate radiation displacement damage (per unit volume, as a function of location) in, e.g., a silicon vertex detector resulting from beam loss nearby or from routine collisions in the interaction region. Outputs from such a calculation (i.e., the non-ionizing energy densities) can then be re-expressed in terms more immediately applicable to a particular device such as the increase in leakage current.[6]

*Fermi National Accelerator Laboratory is operated by Universities Research Association under contract with the US Department of Energy.

This note is a simple extension of the work referred to above. It describes essentially the remaining work necessary to complete the implementation into CASIM of the non-ionizing energy deposition estimation.

2 Calculation

For a given energy and type of particle the non-ionizing energy loss is obtained by calculating the integral

$$(dE/dx)_{n.i.} = N \sum_{Z,A} \int_{E_R^{min}}^{E_R^{max}} (d\sigma/dE_R) T(E_R) dE_R \qquad (1)$$

where N is the number of atoms per unit volume, $(d\sigma/dE_R)$ is the differential cross section for the particle to undergo a collision resulting in a nuclear recoil of kinetic energy E_R. $T(E_R)$ is the so-called Lindhard factor or the total energy lost to non-ionizing processes (atomic motion) by a nucleus of energy E_R. The summation in over Z,A refers to the variety of residual nuclei generated in *inelastic* processes, each with its own $(d\sigma/dE_R)$ and $T(E_R)$, though the dependence of these quantities on Z and A is suppressed in eq. 1 for clarity. The limits of integration are determined by kinematics (E_R^{max}) and by a low-energy cutoff corresponding to the minimum energy required to dislodge a silicon atom from the lattice. An E_R^{min} of 25 eV has been adopted for the results reported here.[3, 4, 6]

Lindhard factors, in a silicon medium, for silicon and for a sampling of nuclides below it in Z and A, as calculated by Lindhard and co-workers are reported in [1]. The striking feature of these curves is that they completely flatten out with increasing energy reaching a plateau around 100 MeV, with about 90% of the plateau value already reached at 10 MeV. For silicon recoils in a silicon medium the plateau value is 300 KeV. The curves in [1] extend down only as far as the 10-40 KeV range. Since this is still far above the adopted threshold of 25 eV the curves were extended downward to threshold using the theoretical nuclear and electronic stopping powers of Lindhard et al. [7]. (A ~10% discrepancy results when the $T(E_R)$ so calculated are compared with those reported in [1]. This is likely due to refinements introduced by Lindhard et al. in their calculation and it is not pursued further here. The $T(E_R)$ used in the present calculation are smoothed over this discrepancy in a manner so as to retain the values of Lindhard et al. in the energy region were they are reported.)

Results of the present calculation are summarized in fig. 1. Below the specific assumptions made in the calculation, sorted by particle type, are briefly discussed. For electrons, muons, and pions the cross sections used in the calculation are averaged over the positive and negative members of the species. The differences between the two are sufficiently small to justify this approximation in the current context.

2.1 Protons

As in [1, 4] the non-ionizing energy loss of protons is the sum of three components: Coulomb, nuclear elastic, and inelastic interactions. For Coulomb scattering the so-called McKinley-Feshbach version of the Rutherford formula is used, which takes acccount of the spin and the sign of the charge of the particle. This must be multiplied by a recoil factor and a nuclear form factor. For the latter a Helm ("gU")-type is used. Details which point to this choice may be found in [8, 9]. By virtue of the threshold in E_R screening corrections may be ignored. Nuclear elastic scattering is assumed to have a total cross section of 220 mb and is represented by a single exponential with a slope fitted to the data of Schiz et al. [10]. The inelastic cross section is taken to be 440 mb. The isotopic distribution of residual nuclei is from Silberberg and Tsao [11] and the associated Lindhard factors are assumed to be the plateau values. This is justifiable in that the kinetic energy of recoil has a Maxwellian type distribution with an average in the 10-20 MeV range [12]. Quasi-elastic scattering, which has a much smaller total cross section, is lumped with the inelastic part. The result, shown in fig. 1, differs slightly from [4].

2.2 Pions

The non-ionizing energy loss of pions is calculated similarly to that for protons. For nuclear elastic scattering the total cross section (112 mb) and exponential slope are also taken from [10]. The total inelastic cross section is assumed to be 371 mb. Since much less data or calculations are available for pions, the simplifying assumption is made that the distribution of the kinetic energy of the residual nuclei and of their isotopic composition is the same as for incident protons which have their kinetic energy augmented by the equivalent of the pion mass.

2.3 Neutrons

The curve of fig. 1 for neutrons is essentially the one from ref. [4] which has been extended from 1 MeV down to 0.1 MeV using the cross section compilation of ref.[13] along with the assumption of isotropic scattering and with the appropriate Lindhard factors. At the high energy end the neutron curve is matched to that for protons minus the Coulomb contribution.

2.4 Photons

For photons the process with the largest cross section is pair production. However, typical nuclear recoils associated with this are very small. This contribution is evaluated using the formulae of Suh and Bethe [14] normalized to the total cross section for *nuclear* pair production.[15] Above about 10 MeV the inelastic nuclear interaction quickly becomes dominant, first via the giant resonance [16] and then via the nucleon isobar resonaces [17] after which the cross section flattens out to ~2.8 mb. Above ~1 GeV a small contribution from coherent production of vector mesons is included. Elastic γA (nuclear Compton) scattering is neglected. The choice of threshold for E_R (25 eV here) may noticeably influence the low energy ($<\sim 10MeV$) regime though not enough to make these contributions significant. In spite of its bumpy appearance the photon curve in fig. 1 incorporates actually considerable smoothing of the basic cross sections.

2.5 Electrons

For electrons only the Coulomb term is assumed present and is treated the same as for protons (but averaged over $e^{\pm}$ here). The large differences between electrons, muons, pions, and protons observed at low energies, where Coulomb scattering dominates over nuclear processes, are almost entirely due to particle mass. (Differences due to spin and charge are negligible by comparison.) At the higher energies the curve in fig. 1 is lower by more than a factor of two compared with its counterpart in [4] due to the inclusion of the nuclear form factor which strongly suppresses large momentum transfers. Inelastic nuclear interaction by the electrons is ignored on the usual grounds that in a thick target the contribution of virtual photons is negligible compared to that of real photons.

2.6 Muons

For completeness the curve for muons is included in fig. 1 although muons will generally contribute very little to radiation damage. Again only the Coulomb part is included in the cross section.

3 Concluding Remarks

As mentioned above there are some differences, most notably for electrons, in the estimates of non-ionizing energy loss between the present calculation and ref. [4]. These differences are not significant enough to impair the conclusion of proportionality between non-ionizing energy deposition and radiation damage. However, they could affect the value of the constant of proportionality (as defined on a 'best fit' basis) for a particular type of device.

As could be anticipated, all curves shown in fig. 1 flatten out above a few GeV. For charged particles the curves of fig. 1 are not evaluated below 1 MeV. In the Monte Carlo it is preferred to treat low energy charged particles by means of the integrals

$$\int_0^{R_0} (dE/dx)_{n.i.}\, dR \quad or \quad \int_0^{E_0} (dE/dx)_{n.i.}/(dE/dx)_{tot}\, dE \qquad (2)$$

where E_0 and R_0 are the kinetic energy and range of the particle. Because of the Coulomb barrier such particles are always introduced into the calculation above a few MeV and for the typical particle the contribution from E below 1 MeV to integrals in eq. 2 does not require very precise treatment. At the present level of approximation, absorption of a stopping π^- on a silicon nucleus is accounted for within the Monte Carlo by depositing an amount of non-ionizing energy equivalent to the inelastic interaction of a $\sim$140 MeV proton at that location.

The calculation of the non-ionizing energy density proceeds much like that of ionization energy deposition. Indeed, it is carried out in parallel with it since the latter (which is essentially the dose in rads or Gray) is useful for many other applications (damage to electronics, heating, etc.). Besides its easy implementation, quoting damage in terms of non ionizing energy density seems somewhat more straightforward than as, e.g., an "equivalent 1 MeV neutron fluence" and it also obviates any worries about the particle direction [18] (which is to be integrated out anyway).

Fig. 1 has important implications for damage to silicon vertex detectors. Because of its proximity to the beams one expects electrons from electromagnetic showers to deliver the dominant share of the rad dose, particularly for the case of nearby beam loss (e.g., on the final focusing quads). However, fig. 1 shows that their contribution to the non-ionizing energy deposition is much lower (by at least a factor of 10) than that of protons or pions which makes for more interesting competition with the hadronic component. It is also evident from fig. 1 that, outside of regions where low energy neutrons are completely predominant, a program such as CASIM (which treats such neutrons rather crudely) can still provide a good estimate of the non-ionizing energy density.

It is a pleasure to thank D. Amidei, E. A. Burke, and G. P. Summers for their helpful comments.

References

[1] G. W. Simon et al., Phys. Rev. **129**, 2454 (1963).

[2] V. A. J. Van Lint et al., IEEE Trans. Nucl. Sci. **NS-22**, 2663 (1975).

[3] E. A. Burke, IEEE Trans. Nucl. Sci. **NS-33**, 1276 (1986); G. P. Summers et al., IEEE Trans. Nucl. Sci. **NS-34**, 1134 (1987).

[4] C. J. Dale et al., IEEE Trans. Nucl. Sci. **NS-35**, 1208 (1988).

[5] A. Van Ginneken, *CASIM. Program to Simulate Hadronic Cascades in Bulk Matter*, Fermilab FN-272 (1975).

[6] see, e.g., several of the contributions in *Radiation Effects at the SSC*, M. G. D. Gilchriese, Ed., SSC-SR-1035 (1988).

[7] J. Lindhard et al., Mat. Fys. Medd. Dan. Vid. Selsk. **33** nr.10 (1963). The 25 eV threshold is taken into account in the extension of $T(E_R)$ but this matters only for E_R close to the threshold value.

[8] R. Herman and R. Hofstadter, *High Energy Electron Scattering Tables*, Stanford University Press, Stanford, CA (1960).

[9] see, e.g., H. Überall, *Electron Scattering from Complex Nuclei*, Academic Press, New York (1971).

[10] A. Schiz, PhD Thesis, Yale University (1979); A. Schiz et al., Phys. Rev. **D21**, 3010 (1980).

[11] R. Silberberg and C. H. Tsao, Ap. J. Suppl. **25**, 315 (1973).

[12] L. Winsberg, Nucl. Inst. Meth. **150**, 465 (1978); —, Phys. Rev. **C22**, 2116 (1980); —, Phys. Rev. **C22**, 2123 (1980).

[13] D. I. Garber and R. R. Kinsey, *Neutron Cross Sections, Vol. II, Curves*, BNL 325 (1976).

[14] K. S. Suh and H. A. Bethe, Phys. Rev. **115**, 672 (1959).

[15] J. H. Hubbell et al., J. Phys. Chem. Ref. Data **4**, 471 (1975).

[16] see, e.g., B. Bülow and B. Forkman, in *Handbook on Nuclear Activation Cross Sections*, pp475-558, IAEA, Vienna (1974).

[17] see, e.g.,*Review of Particle Properties*, Particle Data Group, Phys. Let. B**204**, 1 (1988).

[18] D. E. Groom, Appendix 9 in *Radiation Levels in the SSC Interaction Regions*, D. E. Groom, Ed., SSC-SR-1033 (1988).
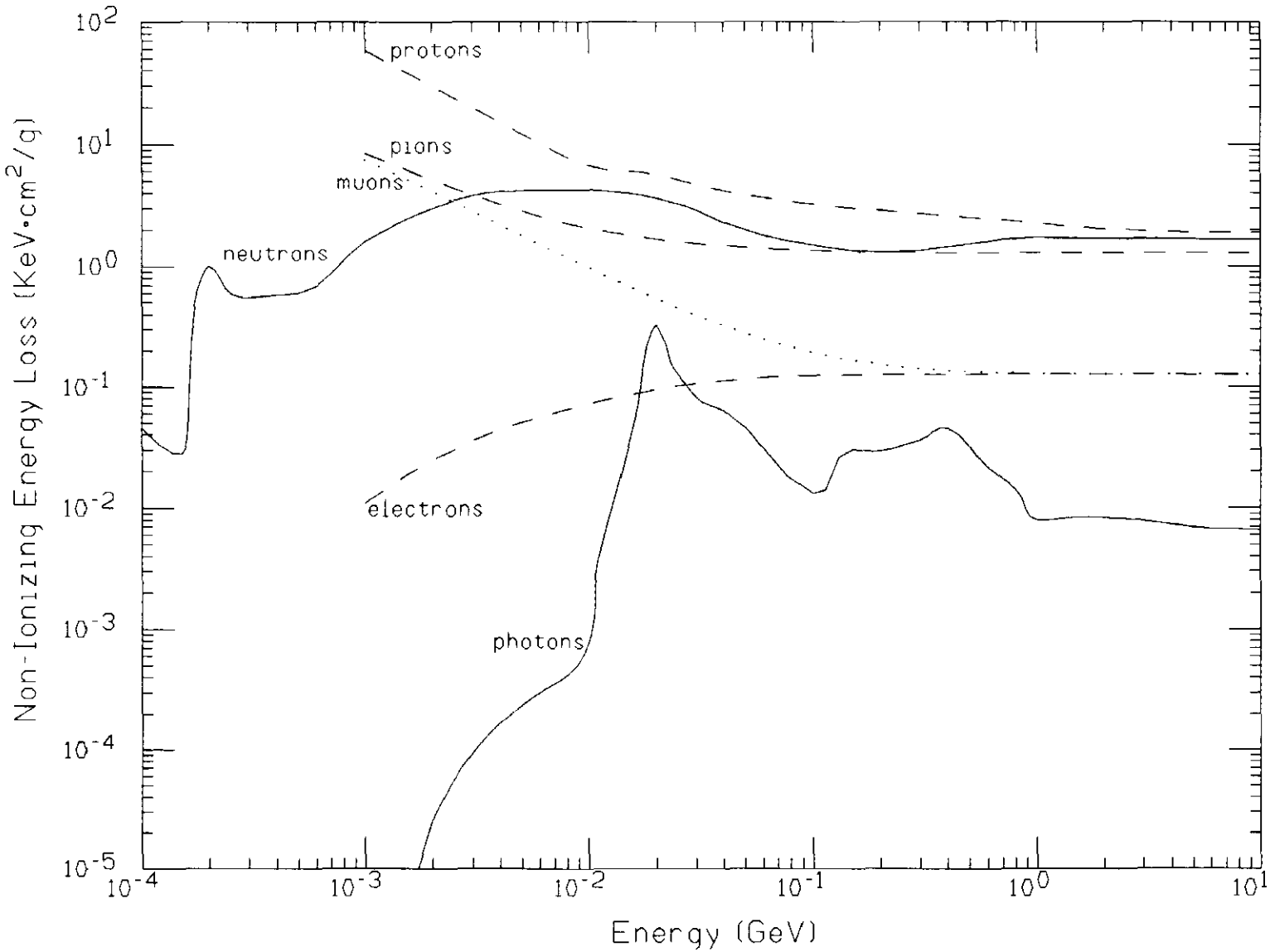
Fig. 1. Non-Ionizing Energy Loss versus Incident Energy